Temperature-Dependent Effects of FeS_2 Thin Film Synthesized by Thermochemical Spraying: An Optical and Physicochemical Investigation

Chia-Tze Kao, Jen-Bin Shi, Hsuan-Wei Lee, Fu-Chou Cheng, Hung-Hsin Liu, Ming-Way Lee, Chih-Chieh Chan, Chien-Wei Huang, et al.

Journal of Thermal Spray Technology

ISSN 1059-9630
Volume 25
Number 3

J Therm Spray Tech (2016) 25:580-586
DOI 10.1007/s11666-016-0379-7

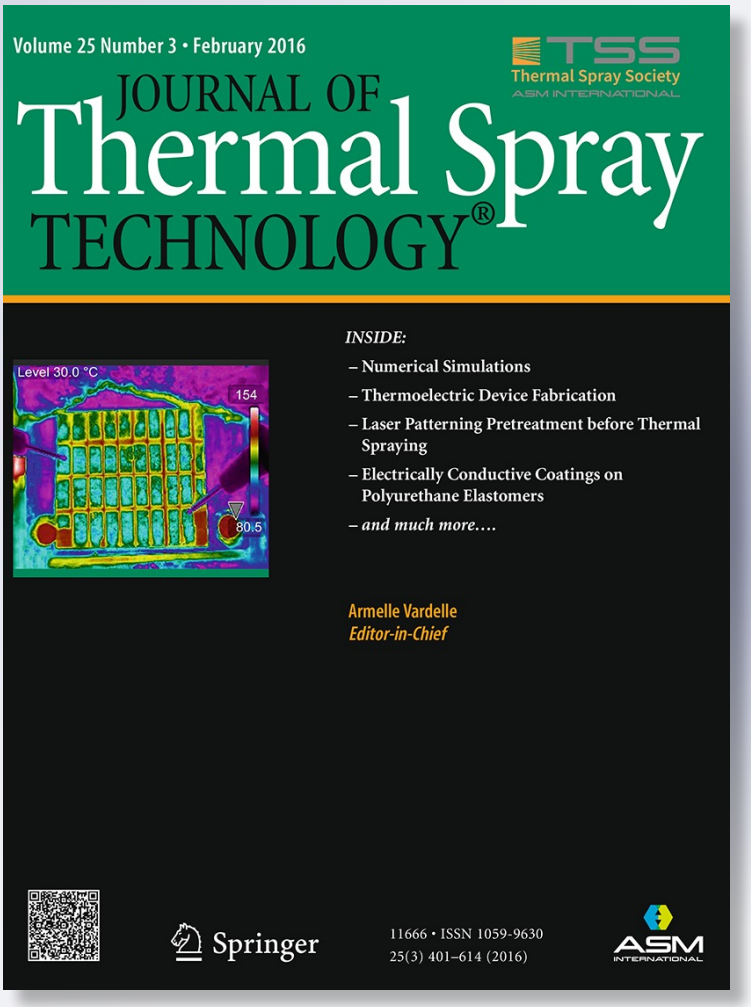

Springer

JTTEE5 25:580–586
DOI: 10.1007/s11666-016-0379-7
1059-9630/$19.00 © ASM International

Temperature-Dependent Effects of FeS_2 Thin Film Synthesized by Thermochemical Spraying: An Optical and Physicochemical Investigation

Chia-Tze Kao, Jen-Bin Shi, Hsuan-Wei Lee, Fu-Chou Cheng, Hung-Hsin Liu, Ming-Way Lee, Chih-Chieh Chan, Chien-Wei Huang, Hsien-Sheng Lin, Po-Feng Wu, Chin-Yi Chen, Ming-Cheng Kao, San-Lin Young, and Cheng-Li Lin

(Submitted March 18, 2015; in revised form November 22, 2015)

FeS_2 pyrite films are used in a variety of applications including solar cells and, the potential scope for their utilization is increasing as their synthetic methods become more economical while maintaining or enhancing their high light absorption coefficients. The glass substrate temperature dependence on the formation of FeS_2 pyrite films was investigated with respect to their optical and physicochemical properties. During the thermochemical spraying process the temperature was varied in the range of 190-290 °C. FeS_2 nanocrystalline (40-70 nm) films, formed as a result of atmospheric spraying with glass substrate temperatures above 260 °C, were observed by SEM. Opto-electronic studies revealed that the nanocrystalline films had a direct band gap (1.3-1.6 eV) with a high light absorption coefficient ($\alpha > 7 \times 10^4$ cm^{-1} for $\lambda < 1800$ nm). Thus, this study offers an alternative to complicated methods for thin-film formation through spaying technology, for the synthesis of high-quality FeS_2 pyrite films with potential application as high light-absorbing solar energy absorbers.

Keywords chemical spray, FeS_2, nanocrystalline films, pyrite, solar energy absorbers

1. Introduction

The cubic system of FeS_2 (pyrite) has attracted great attention as a potential candidate in photo-electrochemical and photovoltaic applications due to its various physicochemical and optical properties. Of these properties, pyrite's major characteristics that make it suitable as an absorber material, for the application in thin-film solar cells, is the high light absorption coefficient ($\alpha > 10^5$ cm^{-1} for $\lambda < 10^3$ nm), suitable energy gap ($E_g = 0.95$ eV), and environmental compatibility (Ref 1-6). In addition, the thickness of pyrite films is only ~10 nm, which usually is able to absorb over 90% sunlight that is allowed to reach the surface of the thin films. However, due to the nature of the pyrite films, the synthesis method is extremely important as it can strongly affect the quality, which influences the physicochemical and optical properties of the final pyrite film. Thus, there is a need for the study of synthesis methods, investigating various parameters such as temperature, reaction time , to improve the efficiency of the solar energy conversion.

Previous studies attempted various methods to prepare pyrite films, such as iron layer evaporation, electro-deposition, electrodeposited iron sulfurization, magnetron sputtering, ion bean magnetron sputtering, metal organic chemical vapor deposition (MOCVD), and spray pyrolysis (Ref 7-13). However, low conversion efficiencies (for example of less that 3%) so far have been unsatisfactory, and the theoretical value has been calculated as much higher than the observed conversion efficiencies. Due to these inefficiencies, further efforts should be attempted in

Chia-Tze Kao, Department of Dentistry, College of Oral Medicine, Chung Shan Medical University, Taichung, Taiwan and Dental Department, Chung Shan Medical University Hospital, No. 110, Sec1, Jianguo N. Rd., Taichung 40201, Taiwan; **Jen-Bin Shi, Chien-Wei Huang,** and **Cheng-Li Lin**, Department of Electronic Engineering, Feng Chia University, No. 100, Wenhwa Rd., Seatwen, Taichung 40724, Taiwan; **Hsuan-Wei Lee, Hsien-Sheng Lin,** and **Po-Feng Wu**, Electrical and Communications Engineering, Feng Chia University, No 100, Wenhwa Rd., Seatwen, Taichung 40724, Taiwan; **Fu-Chou Cheng**, Stem Cell Center, Department of Medical Research, Taichung Veterans General Hospital, No. 160, 3rd Section, Taichung Harbor Rd., Taichung 40705, Taiwan; **Hung-Hsin Liu**, School of Occupational Safety and Health, Chung Shan Medical University, No. 110, Sec1, Jianguo N. Rd., Taichung 40201, Taiwan; **Ming-Way Lee**, Department of Physics, Institute of Nanoscience, National Chung Hsing University, 250 Kuo Kuang Rd., Taichung 40227, Taiwan; **Chih-Chieh Chan**, Department of Chemical Engineering, Feng Chia University, No. 100, Wenhwa Rd., Seatwen, Taichung 40724, Taiwan; **Chin-Yi Chen**, Department of Materials Science and Engineering, Feng Chia University, No. 100, Wenhwa Rd., Seatwen, Taichung 40724, Taiwan; and **Ming-Cheng Kao** and **San-Lin Young**, Department of Electronic Engineering, Hsiuping University of Science and Technology, Taichung 41280, Taiwan. Contact e-mail: jbshi@fcu.edu.tw.

the investigation of low-cost and high-efficiency pyrite films, with interest focused on the potential for electronic and optical applications. Sputtering and MOCVD are the most commonly used in the preparation of FeS_2 thin films, however, the cost of these methods are relatively high in comparison to others. Thus, the low-cost method of spray pyrolysis has received recent attention due to its simplicity, economic feasibility, and potential product commercialization.

These above-mentioned factors have increased the potential of the use of spray pyrolysis in the preparation of FeS_2 thin films, when compared to other methods. The glass substrate temperature has a discernible effect on the opto-electronic and physicochemical properties of these films and thus, during this one-step process the heat energy supplied to the system is important. The method used in this study had no post-annealing treatments, in an attempt to further reduce the manufacturing costs of the FeS_2 pyrite films, as no previous studies have been published to elucidate the effect of temperature on FeS_2 films without post-annealing procedures. Thus, this study focused on the direct formation of spray-deposited FeS_2-thin films at different glass substrate temperatures, and the subsequent effects were thoroughly investigated by structural, compositional, and opto-electronic characterizations to best determine the optimum conditions for synthesis and the relevance for photo-electrochemical and photovoltaic applications.

2. Experimental Details

2.1 Preparation of FeS_2 Thin Films

In this study materials used for the preparation of FeS_2 thin films were all of analytical grade. $FeCl_3$ (SHOWA, Japan) with a purity of 97.0%, CH_4N_2S thiourea purisis with a purity of 98.5% and S sulfur (99.99%) were purchased from Sigma-Aldrich Germany. Distilled water was used throughout this study as the solvent for CH_4N_2S. To produce fine droplets of reactants a spray gun (KUCING BD-130) was used. A Corning CO-PC420D electrical heating plate purchased from Shan Chiou Co. Ltd, Taiwan supplied heat to the glass surface where film formation occurred. A J-type thermocouple purchased from OMEGA Co. Ltd, USA was used as a precision temperature control unit. This study utilizes a laboratory scale spray pyrolysis technique. To execute this spray pyrolysis technique, a modified system was developed and as outlined below (Ref 8). In brief, 50 ml aqueous solution of 0.1 M $FeCl_3$ and 0.6 M thiourea was prepared by dissolving $FeCl_3$ and thiourea in hot distilled water while stirring. After dissolution of the iron and sulfur salts the resulting aqueous solution was then transferred to the spray container (air pressure 10546 kg/m^2 during spraying) and was sealed. This container was then clamped to a stand to assist in a resultant stationary distance of 25 cm between the spray nozzle (diameter 0.3 mm) and glass plate. The spray pyrolysis technique involved a fine mist of reactants from the spray container that had a flow rate of 0.3 ml/min. This fine mist comprised droplets of reactants, thus increasing the probability of uniform deposition of reactants onto the glass plate for homogeneous formation of the thin film. The thermal control of the glass plate, which is necessary for the thermal decomposition and thus removal of volatile compounds, was heated by an electrical heater at the various temperatures of 190, 230, 260, and 290 °C. Each sample was subjected to a different heating temperature and was controlled by the J-type thermocouple, which ensured that temperature fluctuations were limited to ±2 °C. As a result of the evaporation of the volatile compounds the thin films were formed on the top surface of the glass plate.

2.2 Characterization

X-ray diffraction (XRD, Shimadzu, Japan) was used to investigate the crystalline phases present and the percent crystallinity of the films. The x-rays were provided using Cu K_α radiation with the wavelength of 1.54056 Å. Analysis was conducted between the range of 10° to 60° in 2θ mode by increasing the 2θ angle at a rate of 2° per minute, operated at an acceleration voltage of 40 kV and an electron probe current of 30 mA. The FeS_2 thin films formed on the glass plate were also analyzed by Field Emission-Scanning Election Microscopy (FESEM, HITACHI S-4800, Japan) to determine their surface and cross-sectional morphology. In addition, the chemical composition of the surface of the thin films was determined by Energy Dispersive x-ray analysis (EDAX, HITACHI S-4800, Japan). To determine the optical properties of the FeS_2 thin films, optical absorption spectra were recorded in a spectrophotometer (U-3501 spectrophotometer, HITACHI, Japan). The prepared thin films were placed on a clean glass slide designed for the spectrophotometer, which was then positioned into its housing and analysis was then conducted within the wavelength range of 400-1800 nm.

3. Results and Discussion

3.1 Preparation of FeS_2 Thin Films

In this study four thin films were prepared through a modified method of the spray pyrolysis technique. Spray pyrolysis was successfully used to synthesize nanocrystalline iron disulfide pyrite (FeS_2) thin films on glass substrates in aqueous solution using a fixed molar ratio (1:6) of $FeCl_3$ (0.1 M) and CH_4N_2S (0.6 M) respectively. During the preparation of the thin films, it was deduced that through direct preparation of the films, without subjecting the films to any post-annealing treatment, the single-phase pyrite thin-film formation occurred at low substrate temperature, such as 260 and 290 °C.

3.2 Crystal Structure of the Prepared FeS_2 Thin Films

The crystal structure of the prepared FeS_2 thin films was determined by the use of XRD. The x-ray diffractograms of the prepared FeS_2 thin films at the various

substrate temperatures (190, 230, 260, and 290 °C) are shown in Fig. 1 and these diffractograms were interrogated to deduce the characteristics of the nanocrystalline films. At substrate temperature 190 °C, shown in Fig. 1 as FeS_2-190, it was observed that there was incomplete sulfurization of the Fe film and thus resulted in the absence of the characteristic 2θ peak for FeS and FeS_2. The crystal structure of FeS_2-190 was determined to be amorphous. A comparison of the diffractogram at substrate temperature 230 °C, shown in Fig. 1 as FeS_2-230, with FeS_2-190 was done and a similar x-ray pattern was observed. However, at ~ 49.9° for 2θ, there was a weak peak that was absent in the FeS_2-190, thus indicating that during spray pyrolysis at an increased temperature of 230 °C, the FeS (JCPDS 89-6269) thin-film formation started to occur (Ref 9).

The effect of glass substrate temperature was investigated at 260 and 290 °C for the formation of the FeS_2 thin films since at 230 °C there was only minimal formation of FeS as identified initially by the FeS phase. The diffractogram for the glass substrate temperature of 260 °C is shown in Fig. 1 as FeS_2-260, and it was observed from this diffractogram that there was increased formation of FeS. These crystalline peaks at 2θ = 28.6, 33.1, 37.2, 40.9, 47.6, and 56.4 had the corresponding to the hkl indices of (111), (200), (210), (211), (220), and (311), respectively. These peaks were characteristic to the x-ray diffraction peaks of FeS_2 (JCPDS 89-3057). Due to the presence of only FeS_2 in the x-ray pattern and the absence of FeS, as was observed for the glass substrate temperature of 230 °C, it was shown that by increasing the glass substrate temperature to 260 °C there was an increase in the conversion of FeS to FeS_2 for the thin films. Moreover, since the conversion of FeS to FeS_2 was successful at 260°C, the formation of the FeS_2 thin film was also conducted at 290 °C. This thin film was also subjected to XRD interrogation and its corresponding diffractogram is shown in Fig. 1 as FeS_2-290. It was observed from the FeS_2-290 diffractogram that the peaks were similar to the peaks from FeS_2-260, however, all the peaks showed increased intensities at their respective 2θ degrees. However, it should be noted that in the XRD patterns, the presence of the iron disulfide polymorph with an orthorhombic structure was not detectible. Due to these increases in peak intensities it was deduced that the spray pyrolysis technique, at a higher temperature of 290 °C was more effective than at 260 °C, and resulted in the formation of a stronger crystalline structure of the pyrite films. In Fig. 1, the diffraction pattern corresponding to (FeS_2-290) showed the highest peak intensity at 2θ = 33.1° and thus was assigned as the (200) face, based on the hkl index, of the cubic structure of pyrite. The crystalline sizes (D) of the prepared thin films at 260 and 290 °C were determined by Scherrer's formula (Ref 14), shown below in Eq 1, based on the data obtained from the XRD patterns.

$$D = (0.9\lambda)/(\beta\cos\theta) \quad \text{(Eq 1)}$$

where λ is the wavelength of the radiation, β is the broadening of the diffraction peak measured at full width and half of the maximum intensity, and θ is the diffraction angle. These data are shown in Table 1, and from this table it was determined that the crystals were nano-sized, and the effects of the two temperatures on the grain size of the thin films are also shown in Table 1. From this table, it is observed that as the glass substrate temperature increased from 260 to 290 °C, the grain sizes decreased. The decreases in grain size at hkl indices of (111), (200), (210), (211), (220), and (311) corresponded to 3, 4, 10, 4, 13, and 6 nm, respectively.

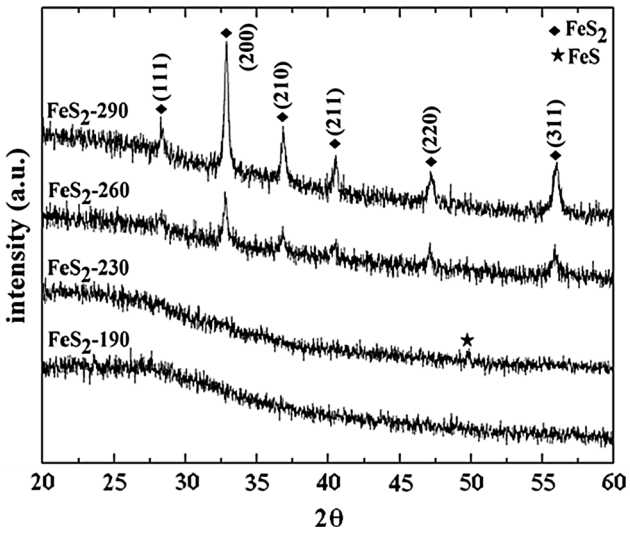

Fig. 1 XRD pattern shows the nanocrystalline Fe-S thin films

3.3 FESEM-EDAX Analysis

The prepared thin films were subjected to FESEM-EDAX analysis and the images are shown in Fig. 2; the EDAX data are presented in Table 2 as a comparison of the Fe and S content of the films. SEM analysis of the thin films prepared at 190 and 230 °C showed that the surface of these films comprised small thin nanorod-like structures projecting out from the surface of the films. The lengths of the nanorods were observed to be between 40 and 70 nm,

Table 1 The dependence of grain size of the thin films at different substrate temperatures

	Grain size, nm at *hkl* index					
Substrate temperature, °C	**(111)**	**(200)**	**(210)**	**(211)**	**(220)**	**(311)**
260	20	24	35	28	32	23
290	17	20	25	24	19	17

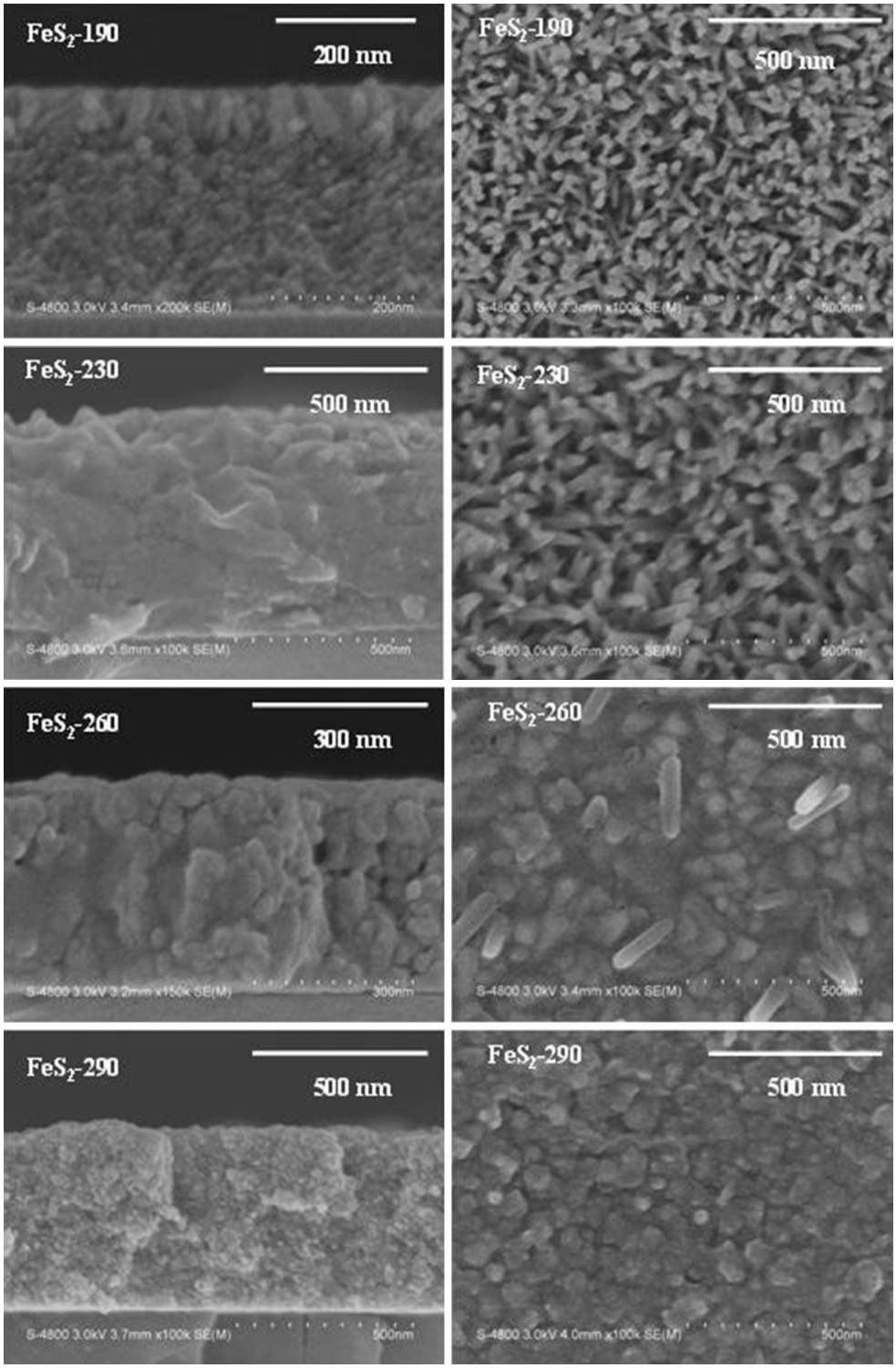

Fig. 2 FESEM images of cross-sectional view and top view of samples at different substrate temperatures

as measured on the surface of the films. As the glass substrate temperature increased from 190 to 230 °C, the thickness of the nanorods increased. In addition, analysis of the cross-sectional view of the thin films at 190 and 230 °C showed that throughout the films the composition was relatively uniform. These nanorod structures were attributed to the reaction initiation of FeS and FeS_2 formation, however, a substantial conversion to FeS_2 was not ob-

Table 2 Surface and cross-sectional of EDAX for the S/Fe atomic ratio of samples with different substrate temperatures

Substrate temperature, °C	Surface	Cross-section
230	1.07	1.05
260	2.09	2.12
290	1.85	1.87

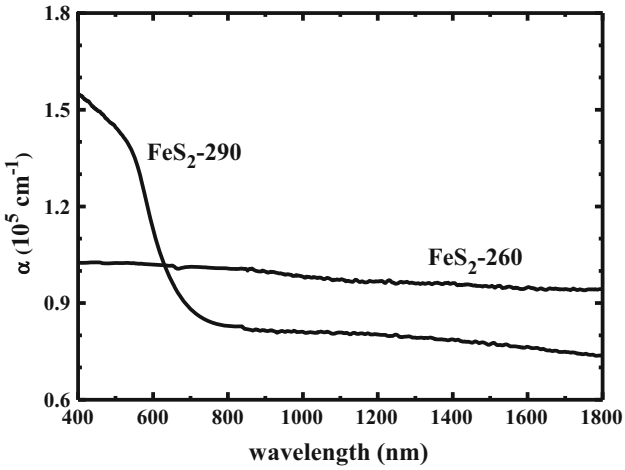

Fig. 3 Plots of absorption coefficients for FeS_2 thin films prepared at different substrate temperatures

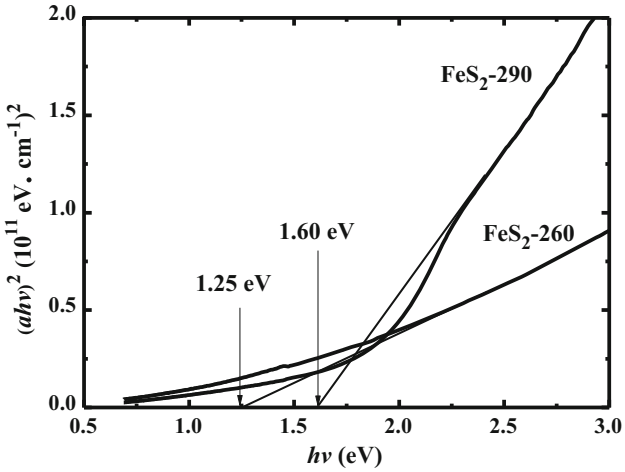

Fig. 4 Plots of $(\alpha h\nu)^2$ vs. $h\nu$ for FeS_2 thin films prepared at different substrate temperatures

served and this deduction was confirmed with the XRD data previously mentioned at $2\theta = 49.9°$.

The films prepared at 260 and 290 °C showed a higher degree of particle aggregation. The films prepared at 260 °C had clearly defined nanorod structures projecting from the surface of the film. However, in comparison to the films formed at 290 °C, nanoparticle aggregates were the dominating morphological feature found on the surface. These structures were attributed to the increased formation of FeS_2 as confirmed in the previous section from the XRD patterns. The increased FeS_2 content of the films prepared at 290 °C may have lead to nanorod aggregation and thus, resulted in the formation of the nano-spherical surface architecture observed for the thin films. In addition, some of these nano-aggregates were also observed in the SEM of the films prepared at 260 °C. To further investigate the morphology of the thin films, the cross-sectional profile was analyzed. The lateral profile of the films prepared at 260 °C was heterogeneous in structure and there was a clear distribution of nano-aggregates in its matrix. However, due to the decrease in grain size from the films prepared at 260 and 290 °C, the lateral profile of the thin films prepared at 290 °C had a higher homogenous character and the differences in the grain size as confirmed by XRD were clearly visible in the SEM images.

The samples observed with FESEM were also analyzed by EDAX to corroborate and understand the surface chemistry of the thin films. The data obtained by the EDAX were evaluated and presented based on the ratios of Fe and S, thus the thin film prepared at 190 °C was not included in this table due to the inefficient formation of FeS and/or FeS_2, and these data are presented in Table 2. The ratios of the surface and cross-sectional elemental composition were evaluated and deduced to be similar with differences of less than 2% (230 °C = ±1.87%, 260 °C = ±1.42% and 290 °C = ±1.07%). Due to the ratios of Fe and S in the thin film prepared at 230 °C, it was seen that the stoichiometry was consistent to the data obtained by the XRD, which indicated that only FeS formation occurred. In addition, the ratios of Fe and S in the thin film prepared at 260 and 290 °C were comparable to the stoichiometric indications as also given by XRD and thus the EDAX analysis was in good agreement to FeS_2 formation.

3.4 Optical Analysis

The optical analysis of the samples was conducted for the thin films with the highest FeS_2 content, prepared at glass substrate temperatures of 260 and 290 °C. The absorption measurements were conducted to determine the absorption coefficients (α) for the two thin films by varying the wavelength from 400-1800 nm and these results are presented in Fig. 3. A high absorption coefficient was observed for the thin film prepared at 290 °C ($\alpha = \sim 1.55 - 0.75 \times 10^{-5}$ cm^{-1}), however, at 260 °C ($\alpha = \sim 1.0 \times 10^{-5}$ cm^{-1}) a lower absorption coefficient was observed. From the UV/Vis absorption spectral data, optical band cap properties of the thin films were calculated using the Tauc's equation. The Tauc's equation is based on the relation of α and photon energy ($h\nu$) as shown in the equation below (Ref 15):

$$(\alpha h\nu)^n = A(h\nu - E_g) \quad \text{(Eq 2)}$$

where h is Plank's constant, n represents the transition, A is a constant, and E_g is the band gap. The n value 2 was chosen to show the direct allowed transition.

The optical band gap of the prepared FeS_2 thin films iss shown in Fig. 4. This band gap relation was made by plotting $(\alpha hv)^n$ versus hv. The value of E_g was obtained by the extrapolation of the sharp linear portion of the graph until the line intercepted the x-axis; this value was then used for E_g. Due to the previously reported transition character of FeS_2, the n value of 2 was selected to represent the direct allowed transition (Ref 4, 16). The band gap of the thin films was determined by extrapolating the linear segments of the plots drawn for $(\alpha hv)^2$ versus hv to obtain the incident energy axis. In this study, the straight line for the determination of the band gap was observed in the range from 2.2 to 3.2 eV and 2.4 to 3.4 eV (data after 3.0 not shown) for the thin films prepared at 260 and 290 °C, respectively.

The observed band gaps are higher than the previously reported direct allowed transition band gap as measured by the Tauc's equation. It was observed that the E_g increased from 1.25 to 1.60 eV as the substrate temperature increased from 260 to 290 °C. The pristine FeS_2 was previously reported to have a eV value of 0.95, however, in this study eV values for the thin film prepared at 260 and 290 °C were 1.25 and 1.60 eV, respectively. This high band gap character was attributed to the epitaxial growth of the nanocrystal, which resulted in the Burstein-Moss effect (Ref 17-19). This effect describes the promotion of the absorption edge to higher energies as the morphological growth of the nanoparticles occurs, due to the population of all states close to the conduction band. In addition, it was speculated that this phenomenon could have been the due to the drastic decrease in grain size of the thin films, which contribute to the quantum energy. The energy level of the system was quantized, and the corresponding band gap was broadened when the grain size was reduced. A previous study deduced that the increased width of the band gap is affected by the electron-hole confinement, and this is most pronounced in a semiconductor quantum dot (Ref 20). Thus, the successfully synthesized thin films at glass substrate temperatures of 260 and 290 °C can be used as the absorbent layer of solar cells, due to the observed band gap of 1.3 and 1.6 eV.

4. Conclusions

This study focused on the synthesis of homogenous FeS_2-pyrite thin films. The method of preparation used four glass substrate temperatures of 190, 230, 260, and 290 °C to evaluate the effect of glass substrate temperature. Physicochemical characterizations determined that the thin films prepared at 260 and 290 °C showed better physicochemical properties. These superior films had good nano-size crystallinity, without the use of post-annealing techniques, and utilized a simple spray pyrolysis method with minimum energy requirements for the low substrate temperatures (<300 °C). The atomic ratios of S/Fe in the thin films prepared at 260 and 290 °C were 2.09 to 2.12 and 1.85 to 1.89, respectively. It was deduced that the atomic ratio of S/Fe greatly decreased from the interstitials of the thin films to the vacant sites of sulfur matrix, as the temperature increased from 260 to 290 °C. These two thin films had high optical absorption coefficients ($\alpha > 7 \times 10^4$ cm^{-1} for $\lambda < 1800$ nm), which resulted in a direct band gap (n = 2). The environmental capability, the band gaps, and the high absorption coefficient observed for these two pyrite films havepromise in the photo-electrochemical and photovoltaic applications via this low-cost method.

Acknowledgments

This research was supported by the National Science Council of R.O.C. under Grant No. NSC-98-2112-M-035-003-MY3, FCU/CSMU-103-2, TCVGH-FCU1038203, and the Precision Instrument Support Center at Feng Chia University.

References

1. A. Ennaoui and H. Tributsch, Energetic Characterization of the Photoactive FeS_2 (pyrite) Interface, *Sol. Energy Mater. Sol. Cells*, 1986, **14**, p 461-474
2. J.R. Ares, A. Pascual, I.J. Ferrer, and C.R. Sanchez, Lattice Intrinsic Defects and Electrical Resistivity in Pyrite Thin Films, *Thin Solid Films*, 2004, **451-452**, p 233-236
3. P.P. Altermatt, T. Kiesewetter, K. Ellmer, and H. Tributsch, Specifying Targets of Future Research in Photovoltaic Devices Containing Pyrite (FeS_2) by Numerical Modeling, *Sol. Energy Mater. Sol. Cells*, 2002, **71**, p 181-195
4. H. Duan, Y.F. Zheng, Y.Z. Dong, X.G. Zhang, and Y.F. Sun, Pyrite (FeS_2) Films Prepared via Sol-Gel Hydrothermal Method Combined with Electrophoretic Deposition (EPD), *Mater. Res. Bull.*, 2004, **39**, p 1861-1868
5. A. Ennaoui, S. Fiechter, H. Tributsch, M. Giersig, R. Vogel, and H. Weller, Photoelectrochemical Energy Conversion Obtained with Ultrathin Organo-Metallic- Chemical-Vapor-Deposition Layer of FeS_2 (Pyrite) on TiO_2, *J. Electrochem. Soc.*, 1992, **139**, p 2514-2518
6. A. Ennaoui, S. Fiechter, Ch Pettenkofer, N. Alonso-Vante, K. Buker, M. Bronold, Ch Hopfner, and H. Tributsch, Iron Disulfide for Solar Energy Conversion, *Sol. Energy Mater. Sol. Cells*, 1993, **29**, p 289-370
7. H. Dahman, M. Khalifa, M. Brunel, and B. Rezig, Iron Pyrite Films Prepared by Sulfur Vapor Transport, *Thin Solid Films*, 1996, **280**, p 56-60
8. R.H. Misho and W.A. Murad, Band Gap Measurements in Thin Films of Hematite Fe_2O_3, pyrite FeS_2 and Troilite FeS Prepared by Chemical Spray Pyrolysis, *Sol. Energy Mater. Sol. Cells*, 1992, **27**, p 335-345
9. M. Bronold, S. Kubala, C. Pettenkofer, and W. Jaegermann, Thin Pyrite (FeS_2) Films by Molecular Beam Deposition, *Thin Solid Films*, 1997, **304**, p 178-182
10. N. Takahashi, T. Yatomi, and T. Nakamura, Crystal Quality, Electrical and Optical Properties of Single Crystal Pyrite Films Prepared by Chemical Vapor deposition under Atmospheric Pressure, *Solid State Sci.*, 2004, **6**, p 1269-1272
11. L. Meng, Y.H. Liu, and L. Tian, Evolutions of Structure, Composition and Optical Absorption Behavior of Pyrite films Formed by Sulfurating Iron, *Mater. Res. Bull.*, 2003, **38**, p 941-948
12. Y.Z. Dong, Y.F. Zheng, H. Duan, Y.F. Sun, and Y.H. Chen, Formation of Pyrite (FeS_2) Thin Nano-films by Thermal-Sulfurating Electrodeposition Films at Different Temperature, *Mater. Lett.*, 2005, **59**, p 2398-2402
13. A. Gomes, J.R. Ares, I.J. Ferrer, M.I. da Silva Pereira, and C. Sanchez, Formation of n-Type Pyrite Films from Electrodeposited Iron Sulphides: Effect of Annealing Temperature, *Mater. Res. Bull.*, 2003, **38**, p 1123-1133

14. K. Manikandan, P. Mani, C.S. Dilip, S. Valli, P.F.H. Inbaraja, and J.J. Prince, Effect of Complexing Agent TEA: The Structural, Morphological, Topographical and Optical Properties of Fe_xS_x Nano Thin Films Deposited by SILAR Technique, *Appl. Surf. Sci.*, 2014, p 76-82
15. J. Tauc and A. Menth, States in the Gap, *J. Non Cryst. Solids*, 1972, **8**, p 569-585
16. G. Smestad, A. Ennaoui, S. Fiechter, H. Tributsch, W.K. Hofmann, M. Birkholz, and W. Kautek, Photoactive Thin Film Semiconducting Iron Pyrite Prepared by Sulfurization of Iron Oxides, *Sol. Energy Mater.*, 1990, **20**, p 149-165
17. K. Sato, Pyrite Type Compounds—With Particular Reference to Optical Characterization, *Prog. Cryst. Sci.*, 1985, p 109-154
18. C. Liu, C. Pettenkofer, and H. Tributsch, Enhancement of Photoactivity in Pyrite (FeS_2) Interfaces by Photoelectrochemical Processes, *Surf. Sci.*, 1988, p 537-554
19. S. Middya, A. Layek, A. Dey, and P.P. Ray, Synthesis of Nanocrystalline FeS_2 with Increased Band Gap for Solar Energy Harvesting, *J. Mater. Sci. Technol.*, 2014, p 770-775
20. T. Takagahara, Effects of Dielectric Confinement and Electron-Hole Exchange Interaction on Excitonic States in Semiconductor Quantum Dots, *Phys. Rev. B*, 1993, **47**, p 4569-4584